

Dear Author

Here are the proofs of your article.

- You can submit your corrections **online**, via **e-mail** or by **fax**.
- For **online** submission please insert your corrections in the online correction form. Always indicate the line number to which the correction refers.
- You can also insert your corrections in the proof PDF and **email** the annotated PDF.
- For **fax** submission, please ensure that your corrections are clearly legible. Use a fine black pen and write the correction in the margin, not too close to the edge of the page.
- Remember to note the **journal title**, **article number**, and **your name** when sending your response via e-mail or fax.
- **Check** the metadata sheet to make sure that the header information, especially author names and the corresponding affiliations are correctly shown.
- **Check** the questions that may have arisen during copy editing and insert your answers/corrections.
- **Check** that the text is complete and that all figures, tables and their legends are included. Also check the accuracy of special characters, equations, and electronic supplementary material if applicable. If necessary refer to the *Edited manuscript*.
- The publication of inaccurate data such as dosages and units can have serious consequences. Please take particular care that all such details are correct.
- Please **do not** make changes that involve only matters of style. We have generally introduced forms that follow the journal's style.
- Substantial changes in content, e.g., new results, corrected values, title and authorship are not allowed without the approval of the responsible editor. In such a case, please contact the Editorial Office and return his/her consent together with the proof.
- If we do not receive your corrections **within 48 hours**, we will send you a reminder.
- Your article will be published **Online First** approximately one week after receipt of your corrected proofs. This is the **official first publication** citable with the DOI. **Further changes are, therefore, not possible.**
- The **printed version** will follow in a forthcoming issue.

Please note

After online publication, subscribers (personal/institutional) to this journal will have access to the complete article via the DOI using the URL:

<http://dx.doi.org/10.1007/s00424-013-1264-6>

If you would like to know when your article has been published online, take advantage of our free alert service. For registration and further information, go to:

<http://www.springerlink.com>.

Due to the electronic nature of the procedure, the manuscript and the original figures will only be returned to you on special request. When you return your corrections, please inform us, if you would like to have these documents returned.

Metadata of the article that will be visualized in OnlineFirst

1	Article Title	Visualization of fast calcium oscillations in the parafascicular nucleus
2	Article Sub- Title	
3	Article Copyright - Year	Springer-Verlag Berlin Heidelberg 2013 (This will be the copyright line in the final PDF)
4	Journal Name	Pflügers Archiv - European Journal of Physiology
5		Family Name Garcia-Rill
6		Particle
7		Given Name Edgar
8		Suffix
9	Corresponding Author	Organization University of Arkansas for Medical Sciences
10		Division Center for Translational Neuroscience, Department of Neurobiology and Dev. Sci
11		Address 4301 W. Markham St., Slot 847, Little Rock 72205, AR, USA
12		e-mail garciarilledgar@uams.edu
13		Family Name Hyde
14		Particle
15		Given Name James
16		Suffix
17	Author	Organization University of Arkansas for Medical Sciences
18		Division Center for Translational Neuroscience, Department of Neurobiology and Dev. Sci
19		Address 4301 W. Markham St., Slot 847, Little Rock 72205, AR, USA
20		e-mail
21		Family Name Kezunovic
22		Particle
23		Given Name Nebojsa
24	Author	Suffix
25		Organization University of Arkansas for Medical Sciences
26		Division Center for Translational Neuroscience, Department of Neurobiology and Dev. Sci

27		Address	4301 W. Markham St., Slot 847, Little Rock 72205, AR, USA
28		e-mail	
29		Family Name	Urbano
30		Particle	
31		Given Name	Francisco J.
32	Author	Suffix	
33		Organization	University of Buenos Aires
34		Division	IFIBYNE, CONICET
35		Address	Buenos Aires, Argentina
36		e-mail	
37		Received	31 December 2012
38	Schedule	Revised	1 March 2013
39		Accepted	7 March 2013
40	Abstract	<p>The parafascicular nucleus (Pf) is an ascending target of the pedunculo-pontine nucleus (PPN) and is part of the “non-specific” intralaminar thalamus. The PPN, part of the reticular activating system, is mainly involved in waking and rapid eye movement sleep. Gamma oscillations are evident in all Pf neurons and mediated by high threshold voltage-dependent N- and P/Q-type calcium channels. We tested the hypothesis that high-speed calcium imaging would reveal calcium-mediated oscillations in synchrony with patch clamp recorded oscillations during depolarizing current ramps. Patch-clamped 9 to 19-day-old rat Pf neurons ($n=148$, dye filled $n=61$, control $n=87$) were filled with Fura 2, Bis Fura, or Oregon Green BAPTA-1. Calcium transients were generated during depolarizing current ramps and visualized with a high-speed, wide-field fluorescence imaging system. Cells manifested calcium transients with oscillations in both somatic and proximal dendrite fluorescence recordings. Fluorescent calcium transients were blocked with the nonspecific calcium channel blocker, cadmium, or the combination of ω-Agatoxin-IVA (AgA), a specific P/Q-type calcium channel blocker and ω-conotoxin-GVIA (CgTx), a specific N-type calcium channel blocker. We developed a viable methodology for studying high-speed oscillations without the use of multi-photon imaging systems.</p>	
41	Keywords separated by ' - '	Arousal - Gamma band activity - Intralaminar thalamus - P/Q-type channels	
42	Foot note information	Francisco J. Urbano and Edgar Garcia-Rill contributed equally as last authors	

The online version of this article (doi:10.1007/s00424-013-1264-6) contains supplementary material, which is available to authorized users.

Electronic supplementary material

ESM 1
(PDF 239 kb)

1
3
2

NEUROSCIENCE

4 **Visualization of fast calcium oscillations**
 5 **in the parafascicular nucleus**

6 **James Hyde · Nebojsa Kezunovic · Francisco J. Urbano ·**
 7 **Edgar Garcia-Rill**

8 Received: 31 December 2012 / Revised: 1 March 2013 / Accepted: 7 March 2013
 9 © Springer-Verlag Berlin Heidelberg 2013

10 **Abstract** The parafascicular nucleus (Pf) is an ascending
 11 target of the pedunculopontine nucleus (PPN) and is part of
 12 the “non-specific” intralaminar thalamus. The PPN, part of
 13 the reticular activating system, is mainly involved in waking
 14 and rapid eye movement sleep. Gamma oscillations are
 15 evident in all Pf neurons and mediated by high threshold
 16 voltage-dependent N- and P/Q-type calcium channels. We
 17 tested the hypothesis that high-speed calcium imaging
 18 would reveal calcium-mediated oscillations in synchrony
 19 with patch clamp recorded oscillations during depolarizing
 20 current ramps. Patch-clamped 9 to 19-day-old rat Pf neurons
 21 ($n=148$, dye filled $n=61$, control $n=87$) were filled with
 22 Fura 2, Bis Fura, or Oregon Green BAPTA-1. Calcium
 23 transients were generated during depolarizing current ramps
 24 and visualized with a high-speed, wide-field fluorescence
 25 imaging system. Cells manifested calcium transients with
 26 oscillations in both somatic and proximal dendrite fluores-
 27 cence recordings. Fluorescent calcium transients were
 28 blocked with the nonspecific calcium channel blocker, cad-
 29 mium, or the combination of ω -Agatoxin-IVA (AgA), a
 30 specific P/Q-type calcium channel blocker and ω -
 31 conotoxin-GVIA (CgTx), a specific N-type calcium channel
 32 blocker. We developed a viable methodology for studying
 33

high-speed oscillations without the use of multi-photon 34
 imaging systems. 35

Keywords Arousal · Gamma band activity · Intralaminar 36
 thalamus · P/Q-type channels 37

Introduction 38 **Q2**

Gamma band oscillations in the cortex appear to participate in 39
 sensory perception, problem solving, and memory [8, 12]. 40
 Cortical interneurons can generate gamma oscillations 41
 through the activation of subthreshold oscillations subserved 42
 by voltage-dependent, persistent sodium channels [25], while 43
 in thalamocortical neurons in “specific” thalamic nuclei, the 44
 mechanism responsible for gamma band activity involves 45
 high threshold, voltage-dependent P/Q-type calcium channels, 46
 which were localized to the dendrites of these neurons using 47
 calcium imaging [33]. Recently, we described the presence of 48
 gamma band activity in nuclei of the reticular activating 49
 system (RAS), specifically, the pedunculopontine nucleus 50
 (PPN) [23], and the “nonspecific” intralaminar thalamic 51
 parafascicular nucleus (Pf) [22]. The role of gamma band 52
 activity in these regions was proposed, rather than participat- 53
 ing in sensory binding, to be involved in the process of 54
 preconscious awareness [10, 44]. The mechanism behind both 55
 PPN and Pf gamma band activity was found to be generated 56
 by P/Q-type calcium channels [22, 23], however, these chan- 57
 nels have never been localized using calcium imaging. The 58
 present study was undertaken to determine if high threshold 59
 calcium channel-dependent membrane oscillations in Pf neu- 60
 rons are localized to the dendrites. 61

The parafascicular nucleus is considered a major compo- 62
 nent of the intralaminar thalamus, which in turn is consid- 63
 ered part of the “nonspecific” thalamocortical system. Pf 64
 neurons send wide-ranging projections to the cortex, stri- 65
 tum, subthalamic nucleus, and substantia nigra [14, 43]. 66

Francisco J. Urbano and Edgar Garcia-Rill contributed equally as last authors

Electronic supplementary material The online version of this article (doi:10.1007/s00424-013-1264-6) contains supplementary material, which is available to authorized users.

J. Hyde · N. Kezunovic · E. Garcia-Rill (✉)
 Center for Translational Neuroscience, Department of Neurobiology
 and Dev. Sci, University of Arkansas for Medical Sciences,
 4301 W. Markham St., Slot 847,
 Little Rock, AR 72205, USA
 e-mail: garciarilledgar@uams.edu

F. J. Urbano
 IFIBYNE, CONICET, University of Buenos Aires, Buenos Aires,
 Argentina

Q1

67	These neurons have long, sparsely branching processes as	oscillations. We were interested in ratiometric measures to	120
68	opposed to the compact, bushy primary dendrites found in	provide an assessment of calcium levels as well as fast imag-	121
69	“specific” thalamocortical (TC) and centrolateral (CL) cells	ing to visualize these rapidly oscillating channels. Further-	122
70	[6, 7]. Some TC neurons present in both the “specific” and	more, we used multiple dyes to provide flexibility to	123
71	“nonspecific” systems possess bushy processes and are	different researchers in the scientific community in relating	124
72	multidendritic with stereotypical intrinsic properties such	these techniques to their experiments. Our results show a	125
73	as bistable states of tonic vs bursting patterns of activity	direct correlation between membrane potential gamma band	126
74	due to the presence of T-current-mediated low threshold	oscillations and intracellular $[Ca^{2+}]$ levels, suggesting that	127
75	spikes (LTS) [26]. This bistable mechanism is considered	gamma oscillations play a central role in the intracellular	128
76	crucial to the cortical synchronization of high-frequency	second messenger pathways of intralaminar thalamic Pf	129
77	rhythms present during waking and rapid eye movement	neurons.	130
78	(REM) sleep (tonic pattern), and synchronization of low-		
79	frequency rhythms during slow wave sleep (LTS bursting).		
80	In vivo electrical stimulation of the CL-Pf nuclei has been	Methods	131
81	shown to generate arousal and gamma band activity (~30–		
82	90 Hz) in the cortical EEG [49]. Pf neurons have also been	Slice preparation	132
83	shown to be involved in maintaining consciousness and		
84	selective attention in primates [28, 34].	All experimental protocols were approved by the Institu-	133
85	We recently reported that all cells in the pedunculopontine	tional Animal Care and Use Committee of the University of	134
86	nucleus (PPN, mainly cholinergic afferents to Pf) can fire at	Arkansas for Medical Sciences, and were in agreement with	135
87	gamma band frequencies, but no higher, when depolarizing	the National Institutes of Health guidelines for the care and	136
88	ramps are applied [23]. Current ramps induced cells to oscil-	use of laboratory animals. Rat pups aged 8–19 days were	137
89	late at gamma band frequencies through specific calcium	taken from adult timed-pregnant Sprague–Dawley rats	138
90	(depolarizing phase of the oscillation) and potassium	weighing 350–380 g. Pups were anesthetized with ketamine	139
91	(repolarizing phase of the oscillation) channels [23]. We also	(70 mg/kg, i.m.) until the tail pinch reflex was absent. Pups	140
92	described similar properties in Pf neurons [22]. High threshold	were decapitated and the brain was rapidly removed and	141
93	P/Q-type calcium channels ($Ca_v2.1$) are present in the den-	cooled in oxygenated sucrose-artificial cerebrospinal fluid	142
94	drites of TC relay neurons. These channels are linked with the	(sucrose-aCSF). The sucrose-aCSF consisted of (in mM):	143
95	generation of gamma band oscillations in the thalamus [24,	sucrose, 233.7; $NaHCO_3$, 26; KCl, 3; $MgCl_2$, 8; $CaCl_2$, 0.5;	144
96	33, 36]. P/Q-type calcium channel knockout animals show	glucose, 20; ascorbic acid, 0.4; and sodium pyruvate, 2. Sag-	145
97	deficits in gamma band generation [24]. N-type calcium chan-	ittal sections (400 μm) containing the Pf nucleus were cut	146
98	nels ($Ca_v2.2$) are found throughout the central nervous sys-	under cooled oxygenated sucrose-aCSF with a Leica	147
99	tem, and animals lacking N-type calcium channels show	VT1200S vibratome (Leica Biosystems, Buffalo Grove, IL)	148
100	deficits in long-term memory and long-term potentiation	with a Huber mini-chiller (Huber, Offenburg, Germany), and	149
101	[18]. Previous work has shown the specific P/Q-type calcium	allowed to equilibrate in normal aCSF at room temperature for	150
102	channel blocker, ω -agatoxin-IVA (AgA), completely	1 h. The aCSF was composed of (in mM): NaCl, 117; KCl,	151
103	abolished calcium oscillations in both Pf and PPN neurons.	4.7; $MgCl_2$, 1.2; $CaCl_2$, 2.5; NaH_2PO_4 , 1.2; $NaHCO_3$, 24.9;	152
104	The specific N-type calcium channel blocker, ω -conotoxin-	and glucose, 11.5. Slices were recorded at 37 °C while being	153
105	GVIA (CgTx), only reduced calcium oscillation amplitude,	superfused (1.5 mL/min) with oxygenated (95 % O_2 and 5 %	154
106	indicating that both voltage-dependent P/Q- and N-type cal-	CO_2) aCSF in an immersion chamber. The aCSF contained	155
107	cium channels may mediate the depolarizing phase of gamma	the following synaptic receptor antagonists: the selective	156
108	band oscillations in both the Pf and PPN [22, 23].	NMDA receptor antagonist 2-amino-5-phosphonovaleric acid	157
109	While we have shown the presence of P/Q- and N-type	(40 μM), the competitive AMPA/kainite glutamate receptor	158
110	calcium channels in Pf neurons, we have not been able to	antagonist 6-cyano-7-nitroquinox-aline-2, 3-dione (1 μM), the	159
111	visually localize these channels. P/Q-type channels are known	glycine receptor antagonist strychnine (10 μM), and the spe-	160
112	to be present in the dendrites of “specific” TC relay neurons	cific GABA _A receptor antagonist gabazine (10 μM).	161
113	[33]. The studies include a method for visualizing and ana-		
114	lyzing high-speed P/Q- and N-type calcium channel-mediated	Whole-cell patch-clamp recordings	162
115	transients in Pf neurons with the goal of determining the		
116	properties calcium transients and their spatial characteristics	Infrared differential interference contrast optics was used to	163
117	during calcium oscillations. We used a combination of Fura 2,	visualize neurons using an upright microscope (Nikon FN-1,	164
118	Bis Fura, and Oregon Green BAPTA 1 because each dye is	Nikon, USA) and QICAM camera (QImaging, Surrey, BC).	165
119	best suited to examining the different aspects of these	A $\times 40$, 0.8 numerical aperture (NA) fluorite water	166

167	immersion objective (Nikon) was used. Whole-cell recordings were performed using borosilicate glass capillaries pulled on a P-97 puller (Sutter Instrument Company, Novato, CA), and filled with EGTA-free, high-K ⁺ intracellular solution, designed to mimic the intracellular electrolyte concentration, composed of (in μM) K-gluconate, 124; HEPES, 40; Mg-ATP, 4; GTP, 0.4 mM; phosphocreatine, 10; and MgCl ₂ , 2. The internal solution was supplemented with Ca ²⁺ sensitive dyes described below. Osmolarity was adjusted to ~270–290 mOsm and pH to 7.3. The pipette resistance was 2–6 M Ω . Previous work showed that oscillations and membrane characteristics were unaffected by pipette resistance within the range of resistances used [22, 23]. All recordings were made using a Multiclamp 700B amplifier (Molecular Devices, Sunnyvale, CA, USA) in current clamp mode. Series resistance and liquid junction potential were compensated for. The average series resistance was 16.7 \pm 0.39 M Ω prior to 35–40 % compensation (>14 KHz). Analog signals were low-pass filtered at 2 kHz, and digitized at 10 kHz using the Digidata-1440A interface and pClamp10 software (Molecular Devices). Holding current of <80 pA was used to maintain resting membrane potential of –50 mV if necessary. The recording region was located immediately anterior and posterior to the middle third of the fasciculus retroflexus (fr). Gigaseal and further access to the intracellular neuronal compartment were achieved in voltage clamp mode, with the holding potential set at –50 mV (i.e., near the resting membrane potential of Pf neurons). Soon after the membrane was ruptured, the intracellular solution and dyes were allowed to equilibrate for 10 min without significant changes in either series resistance (bridge compensation in current clamp mode) or membrane capacitance values before imaging recordings were performed. Experiments lasted between 15 to 25 min from breaking into the cell to experiment completion. Calcium-mediated activity was studied in current clamp mode, in the presence of synaptic blockers (SB, see above) and tetrodotoxin (TTX; 3 μM). Membrane potential was depolarized from –50 mV (a membrane potential known to inactivate T-type calcium channels [22, 23]) using enough current to elicit oscillations, 400–500 pA, 2 s duration ramp current protocols.	218	calcium channel blocker, ω -agatoxin-IVA (AgA; 100–200 nM), a specific P/Q-type calcium channel blocker, and ω -conotoxin-GVIA (CgTx, 1.5–2.5 μM), a specific N-type calcium channel blocker. Blockers were applied for \geq 10 min before testing.	219
171		220		
172		221		
173		222		
174		223		
175		224		
176		225		
177		226		
178		227		
179		228		
180		229		
181		230		
182		231		
183		232		
184		233		
185		234		
186		235		
187		236		
188		237		
189		238		
190		239		
191		240		
192		241		
193		242		
194		243		
195		244		
196		245		
197		246		
198		247		
199		248		
200		249		
201		250		
202		251		
203		252		
204		253		
205		254		
206		255		
207		256		
208	Drug application	257		
209	Bath-applied drugs were administered to the slice via a peristaltic pump (Cole-Parmer, Vernon Hills, IL), and a three-way valve system such that solutions reached the slice 1 min after the start of application. The sodium channel blocker tetrodotoxin citrate (TTX, 3 μM) was purchased from Sigma (St. Louis, MO). Channel blockers were purchased from either Peptide International (Louisville, KY) or Alomone Labs (Jerusalem, Israel). We used cadmium chloride (Cd ²⁺ , 100 μM), a non-specific voltage-dependent	258		
210		259		
211		260		
212		261		
213		262		
214		263		
215		264		
216		265		
217		266		
		267		
		268		
		269		
		270		
		271		
		272		
		273		
		274		
		275		
		276		
		277		
		278		
		279		
		280		
		281		
		282		
		283		
		284		
		285		
		286		
		287		
		288		
		289		
		290		
		291		
		292		
		293		
		294		
		295		
		296		
		297		
		298		
		299		
		300		
		301		
		302		
		303		
		304		
		305		
		306		
		307		
		308		
		309		
		310		
		311		
		312		
		313		
		314		
		315		
		316		
		317		
		318		
		319		
		320		
		321		
		322		
		323		
		324		
		325		
		326		
		327		
		328		
		329		
		330		
		331		
		332		
		333		
		334		
		335		
		336		
		337		
		338		
		339		
		340		
		341		
		342		
		343		
		344		
		345		
		346		
		347		
		348		
		349		
		350		
		351		
		352		
		353		
		354		
		355		
		356		
		357		
		358		
		359		
		360		
		361		
		362		
		363		
		364		
		365		
		366		
		367		
		368		
		369		
		370		
		371		
		372		
		373		
		374		
		375		
		376		
		377		
		378		
		379		
		380		
		381		
		382		
		383		
		384		
		385		
		386		
		387		
		388		
		389		
		390		
		391		
		392		
		393		
		394		
		395		
		396		
		397		
		398		
		399		
		400		
		401		
		402		
		403		
		404		
		405		
		406		
		407		
		408		
		409		
		410		
		411		
		412		
		413		
		414		
		415		
		416		
		417		
		418		
		419		
		420		
		421		
		422		
		423		
		424		
		425		
		426		
		427		
		428		
		429		
		430		
		431		
		432		
		433		
		434		
		435		
		436		
		437		
		438		
		439		
		440		
		441		
		442		
		443		
		444		
		445		
		446		
		447		
		448		
		449		
		450		
		451		
		452		
		453		
		454		
		455		
		456		
		457		
		458		
		459		
		460		
		461		
		462		
		463		
		464		
		465		
		466		
		467		
		468		
		469		
		470		
		471		
		472		
		473		
		474		
		475		
		476		
		477		
		478		
		479		
		480		
		481		
		482		
		483		
		484		
		485		
		486		
		487		
		488		
		489		
		490		
		491		
		492		
		493		
		494		
		495		
		496		
		497		
		498		
		499		
		500		

267 EMBL tools plugin with the simple ratio correction method
 268 [39], applied a 3D median filter [17], and registered with the
 269 Registax plugin [43]. Ratio images were processed with the
 270 Ratio Plus plugin. Image stacks were analyzed in
 271 Metamorph. A 3×3 pixel region of interest were extracted
 272 from each image. Extracted fluorescence recordings were
 273 analyzed in OriginPro (OriginLab Corporation, Northamp-
 274 ton, MA). OGB1 recordings were detrended in OriginPro.

275 Calcium calibration was accomplished with a calibration
 276 buffer kit from Invitrogen (kit C-3008MP), using protocols
 277 outlined by Invitrogen. The kit contains two buffers with
 278 30 mM MOPS at pH 7.2 in 100 mM KCl, one buffer with
 279 39 μM free Ca²⁺ and the other with zero free Ca²⁺. This kit does
 280 not perfectly match the intracellular conditions present, but does
 281 mimic the osmotic and pH of the intracellular solution used and
 282 allows us to confirm the K_d in our system. The kit employs a
 283 reciprocal dilution method to minimize indicator concentration
 284 errors [21, 42]. Each buffer solution was visualized in our
 285 imaging system and fluorescent intensities were recorded.

286 Confocal imaging

287 Upon completing Ca²⁺ imaging, the patch electrode was
 288 carefully removed to maintain cell structure. Slices were
 289 fixed overnight in 4 % paraformaldehyde at 4 °C. The slices
 290 were then washed with 0.1 M phosphate buffer and mounted
 291 with Fluoromount (Sigma). Slices were examined with a
 292 Nikon AZ100 multizoom fluorescence microscope to deter-
 293 mine suitability for confocal scanning. Intact neurons were
 294 scanned on a Zeiss PASCAL LSM 5 confocal microscope
 295 (Oberkochen, Germany) with a ×40 0.8 NA objective.
 296 Alexa-594 was illuminated with 543 nm excitation light.
 297 Image stacks were acquired at 1,024×1,024 with ×4 aver-
 298 aging. Stacks were deconvoluted and processed with Amira
 299 software (Visualization Sciences Group, Burlington, MA).

300 Data analysis

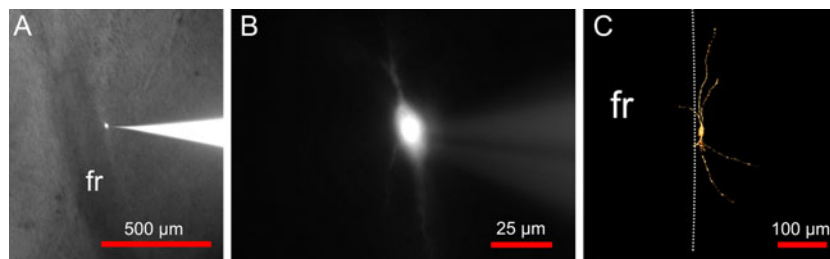
301 Off-line analyses were performed using Clampfit software
 302 (Molecular Devices). Comparisons between groups were

303 carried out using Student's *t* test and ANOVA with 303
 304 Bonferroni post hoc testing using OriginPro. ANCOVA 304
 305 tests were performed with Prism (Graphpad, La Jolla, CA). 305
 306 Power spectra were compiled from current clamp recordings 306
 307 using ramps. All data were tested for normality using the 307
 308 D'Agostino-Pearson omnibus test and was normally dis- 308
 309 tributed ($P \geq 0.05$). Fluorescence curve areas were calculat- 309
 310 ed for the full record using the integration function in 310
 311 OriginPro. Differences were considered significant at 311
 312 values of $P \leq 0.05$. All results are presented as means±SE. 312

313 Results

314 Whole cell patch-clamp recordings were conducted on a 314
 315 total of 148 Pf neurons. Calcium transients were recorded 315
 316 in 61 of these neurons while 87 were recorded without 316
 317 calcium dyes. All neurons were localized as previously 317
 318 described [22, 46]. Cells were localized immediately ante- 318
 319 rior or posterior to the *fasciculus retroflexus* (*fr*) (Fig. 1a). 319
 320 Cells were mainly spindle-shaped and possessed sparsely 320
 321 branching bipolar dendrites (Fig. 1b). Cells were 321
 322 recorded regardless of the presence or absence of LTS 322
 323 currents as depolarizing current ramps were applied from 323
 324 membrane potentials known to prevent the activation of 324
 325 these currents, which are known to be activated at much 325
 326 more hyperpolarized membrane potentials [22, 23]. 326

327 Previous work showed no difference in resting membrane 327
 328 potential between Pf cells with LTS and those that lacked LTS 328
 329 [22]. More depolarizing average resting membrane potential 329
 330 values were observed for higher affinity Ca²⁺ dyes (see cali- 330
 331 bration curves below; OGB1 -44±2 mV, $n=19$; Fura 2 -48± 331
 332 1 mV, $n=25$; Bis Fura -50±2mV $n=17$), showing significant 332
 333 differences only between OGB1 and Bis Fura (ANOVA, $F_{2,}$ 333
 334 $_{58}=5.61$, $P=0.006$; Fura 2 vs. OGB1, $P=0.076$; Bis Fura vs. 334
 335 OGB1, $P=0.005$; Fura 2 vs. Bis Fura, $P=0.646$), and between 335
 336 dye groups and control cells (CTRL -56.3±0.88 mV, $n=87$; 336
 337 Fura 2 vs. CTRL, $P=2.4 \times 10^{-8}$; Bis Fura vs. CTRL, $P=5.8 \times$ 337
 338 10^{-4} , OGB1 vs. CTRL, $P=4.8 \times 10^{-13}$). We studied the pres- 338
 339 ence of fluorescent calcium oscillations in the cell soma and 339



Q3 **Fig. 1** Localization and morphology of Pf neurons. **a** Location of a single recorded neuron immediately posterior to the fasciculus retroflexus (*fr*) in a parasagittal thalamic section (*bright field*). **b** Wide field fluorescence image of the same neuron identified with

intracellular injection of Alexa Fluor 594. Note the sparsely branching processes. **c** Maximum projection confocal image of an Alexa Fluor 594 filled neuron. Long, sparsely branching processes are present

340 proximal dendrites in relation to depolarizing current ramps.
 341 We further characterized the fluorescent calcium oscillations
 342 with the application of broad as well as specific voltage-
 343 dependent calcium channel blockers. Finally, we tested the
 344 fluorescent calcium oscillations in the presence and absence of
 345 TTX.

346 Calibration

347 In order to determine the differential affinity for intracel-
 348 lular calcium concentration $[Ca^{2+}]$ by Fura 2, Bis Fura,
 349 and OGB, K_d values for each dye were analyzed using
 350 calcium calibration buffers. The calibration curves were
 351 averages of four calibration experiments performed with
 352 Fura and Bis fura and six experiments for OGB1 for
 353 each $[Ca^{2+}]$ (see supplemental Fig. 1). OGB1 showed
 354 the highest affinity with a $K_d=210\pm 10$ nM, followed
 355 by Fura 2 with a $K_d=322\pm 8$ nM. As expected, Bis Fura
 356 had the lowest affinity $K_d=885\pm 6$ nM. It should be
 357 noted, that some non-linearity was present in the calibra-
 358 tion curves toward saturating calcium concentrations. If
 359 the saturation values are ignored, the K_d for OGB1 and
 360 Bis Fura was close to the manufacturer specified values.

361 Depolarizing ramps generated calcium transients in Pf 362 neurons

363 We tested the hypothesis that in the presence of TTX and
 364 synaptic blockers, depolarizing current ramps will induce
 365 measureable calcium transients. Each patched neuron was
 366 depolarized with a current ramp in current clamp mode,
 367 which induced calcium oscillations regardless of dye
 368 (Fig. 2a, black records). Frequencies ranged from beta
 369 (13–20 Hz) to low gamma (20–40 Hz). Fluorescence traces
 370 showed an increase in $\Delta F/F$ coinciding with the increase in
 371 current (Fig. 2c, black records). Blocking P/Q-, N-, and T-
 372 type calcium channels with the non-specific calcium chan-
 373 nel blocker Cd^{2+} completely eliminated calcium oscillations
 374 in the electrical recording (Fig. 2, red records) and calcium
 375 transients in the fluorescence recording.

376 The average integrated curve area of fluorescence tran-
 377 sients recorded in both the soma (Fura 2 104 ± 14.3 , $n=10$;
 378 Bis Fura 37 ± 11 , $n=5$; OGB1 124 ± 39 $\Delta F*\text{ms}$, $n=6$) and
 379 proximal dendrite (Fura 2 70 ± 9.2 , $n=7$; Bis Fura 24 ± 4 ,
 380 $n=5$; OGB1 62 ± 15 $\Delta F*\text{ms}$, $n=13$) decreased significantly
 381 for both the soma recordings (Fura 2 32 ± 9.8 , $P=0.027$; Bis
 382 Fura 10 ± 8.9 , $P=0.026$; OGB1 7 ± 1.3 $\Delta F*\text{ms}$, $P=0.032$), and
 383 dendrite recordings (Fura 2 23 ± 1.3 , $P=0.001$; Bis Fura $8.8\pm$
 384 0.7 , $P=0.034$; OGB1 5 ± 0.6 $\Delta F*\text{ms}$, $P=0.002$) using a Stu-
 385 dent's t test (Fig. 2d, e). Ratiometric measurements, converted
 386 to calcium concentrations using calibration curves, showed
 387 resting concentrations of 41 ± 26 nM, somatic ($n=10$) and $62\pm$
 388 14 nM, dendritic ($n=11$) for Fura 2, and 45 ± 20 nM, somatic

($n=6$) and 51 ± 23 nM, dendritic ($n=5$) for Bis Fura. The
 calcium transients showed a peak of 137 ± 39 , somatic
 and 90 ± 15 , dendritic for Fura 2 and 82 ± 49 , somatic
 and 53 ± 22 dendritic for Bis Fura. Please note that absolute
 calcium concentrations are tentative since the effects of
 the unique intracellular environment can widely affect
 the dye K_d values.

We also examined the fluorescent calcium transients
 using synaptic blockers only, and omitting TTX. We tested
 whether the fluorescence curve area decreased when TTX
 was omitted, causing calcium channels to be inactivated by
 unclamped nearby synaptic neuronal activity as well as by
 recurrent over-activation of Pf dendritic compartments.
 While the fluorescence curve area appears slightly smaller
 when comparing synaptic blockers with and without TTX
 for each dye (Figs. 3 and 4d, e), the differences were not
 statistically significant (Fura 2 $P=0.866$, Bis Fura $P=0.096$,
 OGB1 $P=0.22$). Also, while the cells recorded with synaptic
 blockers only appeared to have higher oscillation frequen-
 cies (Fig. 3b), the mean peak oscillation frequencies were
 not statistically different (Fura 2 $P=0.25$, Bis Fura $P=0.154$,
 OGB1 $P=0.088$). The average integrated curve areas for
 both the soma (Fura 2 85 ± 17.1 , $n=5$; Bis Fura 72 ± 13.7 ,
 $n=6$; OGB1 55 ± 21.7 , $n=4$) and proximal dendrite (Fura 2
 27 ± 3 , $n=8$; Bis Fura 27 ± 2.6 , $n=9$; OGB1 12 ± 2.1 , $n=15$)
 showed a significant decrease in fluorescence when Cd^{2+}
 was bath-applied for both soma (Fura 2 36 ± 5.1 , $P=0.016$;
 Bis Fura 26 ± 4 , $P=0.007$; OGB1 5 ± 0.6 , $P=0.0467$) and
 proximal dendrite areas (Fura 2 16 ± 2.7 , $P=7.5\times 10^{-4}$; Bis
 Fura 13 ± 0.98 , $P=6.3\times 10^{-4}$; OGB1 5 ± 0.9 , $P=4.4\times 10^{-4}$).

Effects of specific calcium channel blockers on Pf fluorescent calcium transients

Our previous work has shown that calcium oscillations in
 the Pf are due to P/Q- and N-type voltage-dependent
 calcium channels [22]. We studied the effects of both
 AgA (a specific P/Q-type calcium channel blocker,
 200 μM) and CgTx (a specific N-type calcium channel
 blocker, 1.5–2.5 μM) in order to confirm that P/Q- and
 N-type calcium channels are responsible for the observed
 fluorescent calcium transients ($n=19$). The combination
 of AgA and CgTx completely abolished electrical oscil-
 lations (Figs. 3 and 4a, b, red records) as well as calcium
 transients (Figs. 3 and 4c, red records). The average
 integrated fluorescence curve areas for soma (Fura 2
 105 ± 14.5 , $n=5$; Bis Fura 83 ± 19.3 , $n=6$; OGB1 $77\pm$
 26.2 , $n=6$) and proximal dendrite (Fura 2 $26\pm 12.77.1$,
 $n=7$; Bis Fura 27 ± 3.5 , $n=9$; OGB1 18 ± 5.4 , $n=13$)
 showed a significant decrease in both the soma (Fura 2 $33\pm$
 9.8 , $P=0.027$; Bis Fura 31 ± 19.3 , $P=0.048$; OGB1 7 ± 2.9 ,
 $P=0.047$) and proximal dendrite (Fura 2 16 ± 2.4 , $P=1.7\times 10^{-4}$;
 Bis Fura 14 ± 2.8 , $P=3.4\times 10^{-4}$; OGB1 3 ± 0.5 , $P=0.008$).

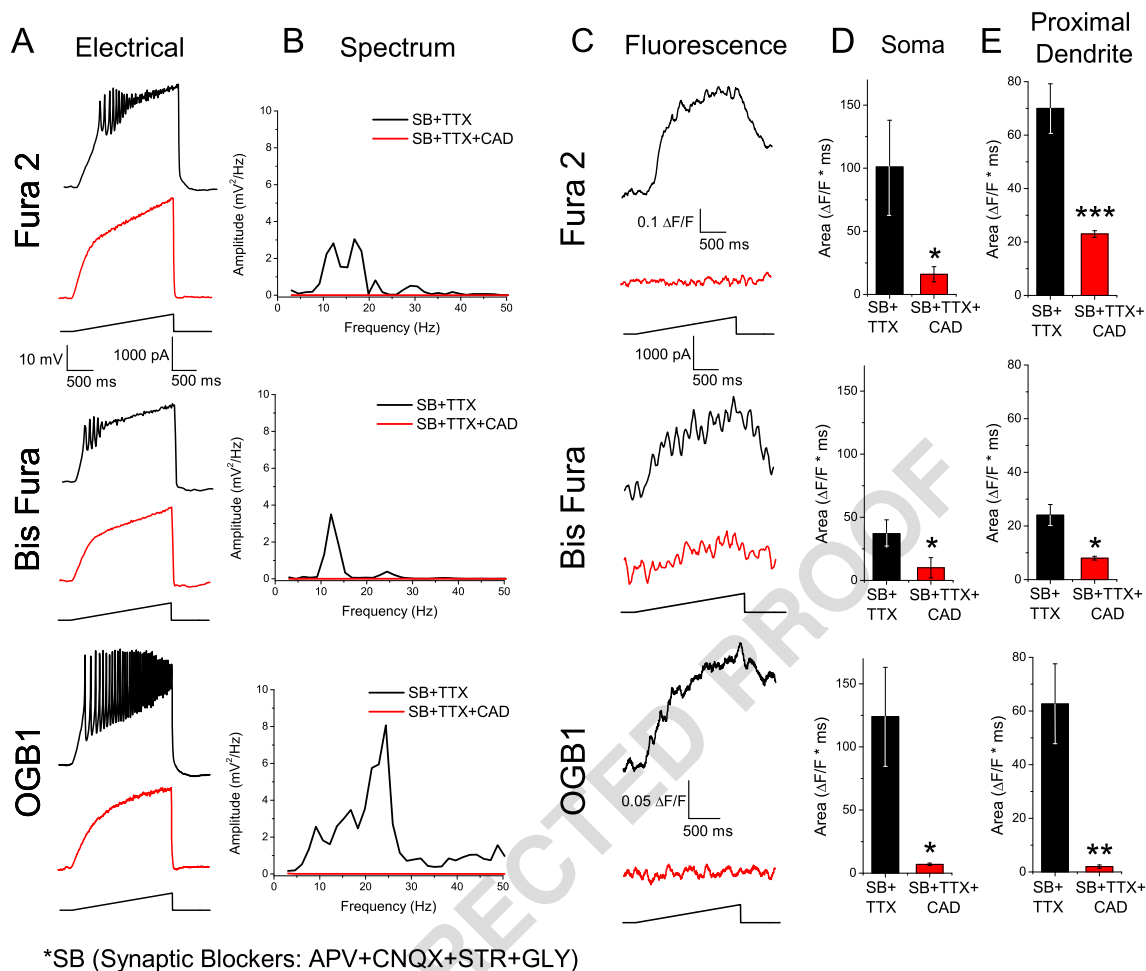


Fig. 2 Depolarizing current ramps generated oscillations and measurable intracellular calcium transients. **a** Representative oscillations of a Pf neuron (*black recording*) and in the presence of CdCl₂ (100 μM; CAD; *red recordings*) obtained during 2 s long ramps. **b** Overlapping recordings comparing power spectrum amplitudes for oscillations present in (**a**), before and after CAD. **c** Somatic fluorescent transients induced by the current ramp (*black record*), recorded simultaneously with the oscillations present in (**a**). Note how both membrane oscillations and intracellular calcium fluorescence signals

were eliminated after CAD (*red record*). **d** Bar graph showing the average integrated somatic curve area for the fluorescence curves before CAD (*black bar* Fura 2 104±14.3, Bis Fura 37±11, OGB1 124±39 ΔF*ms) and after CAD (*red bar* Fura 2 32±9.8, Bis Fura 10±8.9, OGB1 7±1.3 ΔF*ms). **e** Bar graph showing the average integrated proximal dendritic curve area for the fluorescence curves before CAD (*black bar* Fura 2 70±9.2, Bis Fura 2±4, OGB1 62±15 ΔF*ms) and after CAD (*red bar* Fura 2 23±1.3, Bis Fura 8.8±0.7, OGB1 5±0.6 ΔF*ms). *P<0.05; **P<0.01; ***P<0.001

440 Calcium oscillations were evident in the calcium-dependent
 441 fluorescence signal

442 We used OGB1 to record calcium transients at higher frame
 443 rates in order to test the hypothesis that calcium oscillations
 444 recorded in the electrical patch recordings would also be pre-
 445 sent in fluorescent calcium recordings. We observed simulta-
 446 neous oscillations in both patch and fluorescent records in 11
 447 OGB1 filled neurons. In Fig. 5, the electrical recording is
 448 shown in the black record in part A. Fluorescence was recorded
 449 from the soma and two proximal dendrite branches (red, pink,
 450 and green records). The red somatic fluorescence record shows
 451 peaks that match each oscillation peak in the black electrical
 452 record, although the fluorescence peaks had a slight delay in
 453 comparison to the electrical peaks (Fig. 5b, ~10 ms delay

initially and decreased with each successive oscillation). The
 dendrite records (pink and green records) show oscillations that
 matched the electrical record. Some oscillation peaks can be
 seen on dendrite 1, but not on dendrite 2 and vice versa. Some
 oscillation peaks were present in both dendrite records while
 others present in the dendrite records may not be evident in the
 electrical record. It must be noted that the electrical record is
 from the soma and represents a sum of all activity in the cell, in
 particular a sum of calcium activity in all of the dendrites.
 Cross-correlation analysis of the electrical and somatic fluores-
 cence records (Fig. 5c) indicated a 12-ms lag with a frequency
 of approximately 15 Hz. This is also supported by the power
 spectrum (Fig. 5c), with the somatic fluorescence signal show-
 ing a broad peak centered at 14 Hz (red line) which matches the
 15 Hz peak in the electrical record (black line).

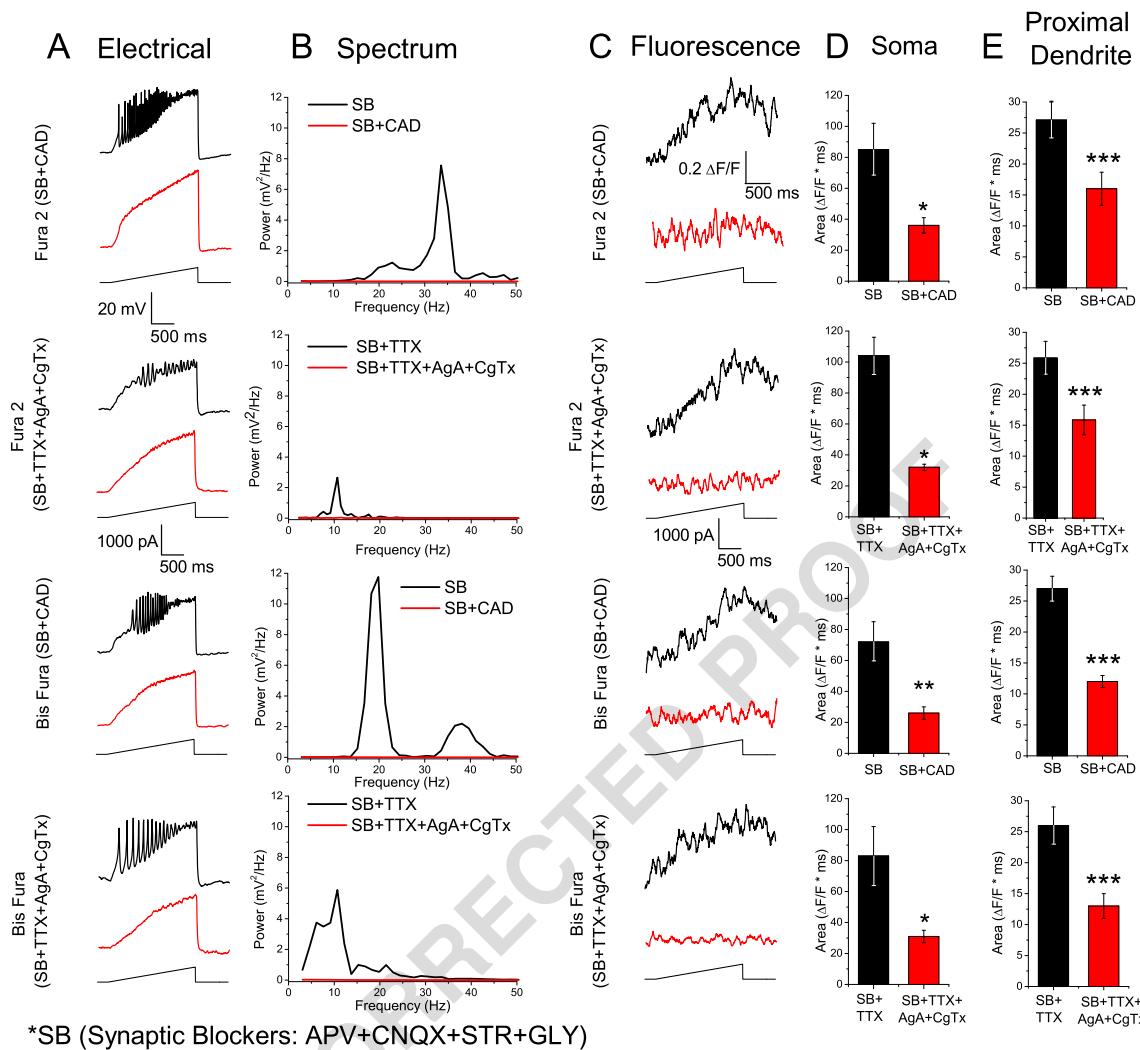


Fig. 3 N- and P/Q-type calcium channels mediate calcium oscillations in the Pf visualized with Fura 2 and Bis Fura. SB (synaptic blockers). **a** Representative calcium oscillations with and without TTX (*black record*) and after bath application of specific calcium channel blockers AgA and CgTx or the nonspecific calcium channel blocker CAD (*red record*). Note that calcium oscillations were eliminated by AgA and CgTx, indicating fluorescence (**c**) was mediated by N- and P/Q-type calcium channels. **b** Power spectrum of records shown in (**a**). **c** Somatic fluorescence signals recorded simultaneously with oscillations in (**a**). **d** Bar graph showing the average integrated somatic curve area for the fluorescence curves before AgA and CgTx (*black bar* Fura 2 105±

14.5, Bis Fura 83±19.3 ΔF*ms) and after AgA and CgTx (*red bar* Fura 2 33±9.8, Bis Fura 31±19.3 ΔF*ms). Synaptic blocker only conditions before CAD (*black bar* Fura 2 85±17.1, Bis Fura 72.3±13.8 ΔF*ms) and after CAD (*red bar* Fura 2 36.4±5.1, Bis Fura 26±4 ΔF*ms). **e** Bar graph showing the average integrated proximal dendritic curve area for the fluorescence curves before AgA and CgTx (*black bar* Fura 2 26±12.77.1, Bis Fura 27±3.5 ΔF*ms) and after AgA and CgTx (*red bar* Fura 2 16±2.4, Bis Fura 14±2.8 ΔF*ms). Synaptic blocker only conditions before CAD (*black bar* Fura 2 27.1±3, Bis Fura 27±2.7 ΔF*ms) and after CAD (*red bar* Fura 2 16±2.7, Bis Fura 12.9±0.98 ΔF*ms) *P<0.05; **P<0.01; ***P<0.001

469 The full calcium transient showed a graded response
470 (Fig. 6b) as the fluorescence signal was measured sequentially
471 across 50 μm of proximal dendrite in 5 μm steps (Fig. 6a).
472 Oscillations were conserved along the length of the dendrite
473 with few gaps. The calcium flux dropped rapidly in the first
474 30 μm of dendrite but began to level off after (Fig. 6c).

475 Characterization of oscillation frequency and age dependence

476 The peak oscillation frequency was plotted against age of
477 each fluorescent cell (Fig. 7c). Linear regression was

performed on each dye group. While Fura 2 and Bis Fura 478
479 labeled cells decreased in oscillation frequency with age,
480 OGB1 cells increased in oscillation frequency with age.
481 ANCOVA analysis showed that none of these trend lines
482 were significantly different. An age/frequency plot of the
483 control cells (which lacked any calcium dye) showed an
484 increase in frequency as age increased (Fig. 7a). This is in
485 agreement with our previously published results showing
486 that, early in Pf development, the maximum oscillatory
487 frequency is in the alpha and beta ranges and gradually
488 increases and plateaus in the gamma range with age [22].

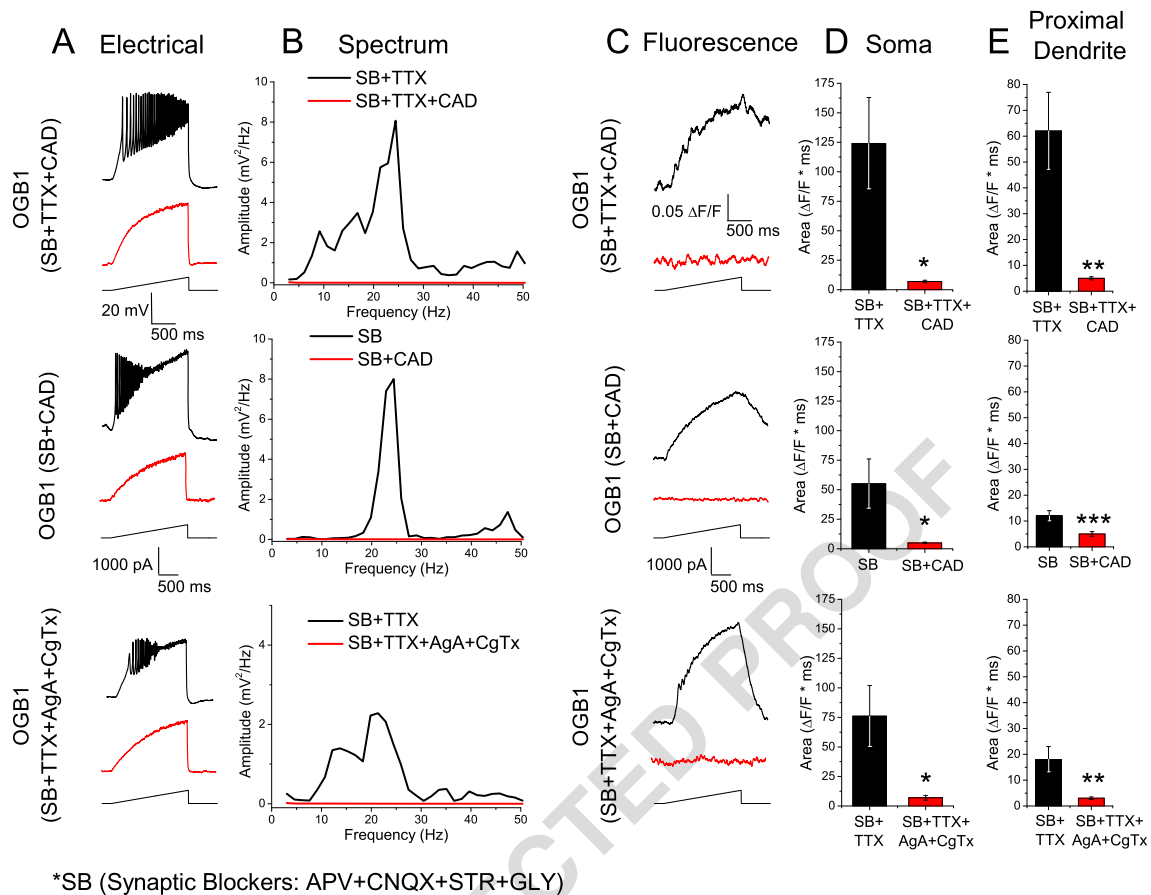


Fig. 4 N- and P/Q-type calcium channels mediate calcium oscillations in the Pf visualized with OGB1. **a** Patch clamp recorded calcium oscillations before (black record) and after (red record) specific and nonspecific calcium channel blockers. **b** Power spectra of records in (a). **c** Fluorescence recordings acquired simultaneously with electrical recordings in (a), with (red record) and without (black record) calcium channel blockers. **d** Bar graph showing the average integrated somatic curve area for the fluorescence curves before CAD (black bar SB only

55.5±21.6, with TTX 124±39 ΔF*ms) and after CAD (red bar SB only 5.5±0.65, with TTX 7±1.3 ΔF*ms). Before AgA and CgTx (black bar 77±26.2 ΔF*ms) and after (red bar 7±2.9 ΔF*ms). **e** Bar graph showing the average integrated proximal dendritic curve area for the fluorescence curves before CAD (black bar SB only 12.5±2.1; with TTX 62±15 ΔF*ms) and after CAD (red bar SB only 5±0.94, with TTX 5±0.6 ΔF*ms). Before AgA and CgTx (black bar 18±5.4 ΔF*ms) and after (red bar 3±0.5 ΔF*ms)

489 Cells were divided into two age groups; 9–14 days old and
 490 15–19 days old (Fig. 7b). The mean peak frequency of
 491 oscillations in Fura 2 filled cells in the two age groups
 492 were compared (9–14 DO 19±1.4 Hz, n=16; 15–19 DO
 493 15±0.94 Hz, n=9) and were not significantly different
 494 (P=0.059). Bis Fura filled cells were not compared due
 495 to too few cells in the 15–19 DO age group. OGB1
 496 filled cells (9–14 DO 21±1.7 Hz, n=12; 15–19 DO 19±
 497 3.7 Hz, n=7) displayed no significant difference between
 498 groups (P=0.583). Control cells (9–14 DO 34±2.1 Hz,
 499 n=53; 15–19 DO 49±2 Hz, n=34) displayed a signifi-
 500 cant difference between age groups (P=1.4×10⁻⁵).

501 The mean peak frequency of dye filled cells in each age
 502 group was compared to control cells (Fig. 7d). The Fura 2
 503 and OGB1 peak frequencies in the 9–14 DO age group were
 504 significantly lower than the control frequency (Fura 2 vs.
 505 CTRL, P=1.9×10⁻⁴; OGB1 vs. CTRL, P=3.4×10⁻⁶). Both
 506 Fura 2 and OGB1 peak frequencies were significantly lower

than the control frequency in the 15–19 DO age group (Fura 2 vs. CTRL, P=1×10⁻⁸; OGB1 vs. CTRL, P=0.003). This indicates that all of the calcium dyes decreased oscillation frequencies, possibly due to the calcium buffering effects of the dye. Averaged power spectra for each group are provided in supplemental Fig. 2. We should note that TTX decreased oscillation amplitude. This has been observed in our previous studies and was attributed to the lack of high-frequency action potentials and the associated decrease in synaptic activity.

Discussion

517 The present study generated the following important origi-
 518 nal findings. (1) Ratiometric analyses using two separate
 519 calcium dyes revealed that calcium concentrations increased
 520 in Pf dendrites in parallel with the electrical signal from the
 521

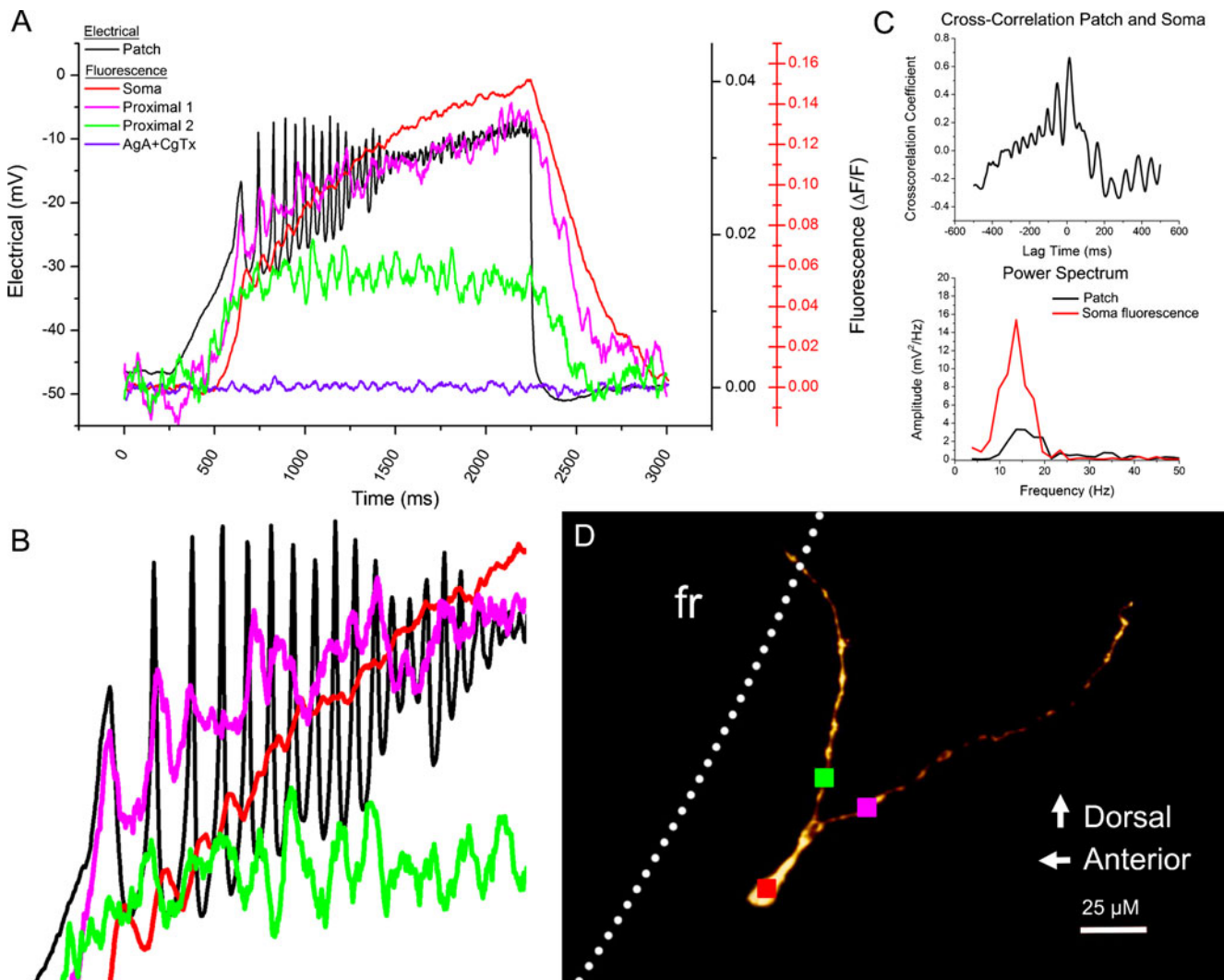


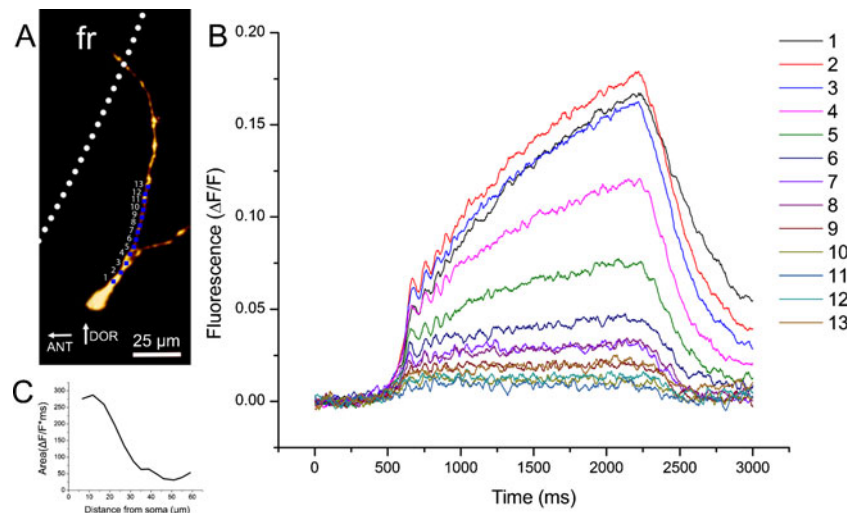
Fig. 5 Oscillations present in the electrical patch-recorded signal were also evident in the recorded calcium signal. **a** Overlay of the electrical patch signal (*black record*) with the somatic calcium signal (*red record*) and calcium recordings from two dendritic branches (*pink and green*, sampling locations shown in **d**). The somatic calcium signal after AgA and CgTx application is shown in *red*. Note that the somatic calcium signal uses a different *y*-axis scaling (*red*). **b** Zoom of the

oscillation signal in **a**). A slight time delay (~ 10 ms and decreasing) is present in the somatic signal. Some oscillations were present in dendritic signals that matched the electrical signal while others were slightly out of phase. **c** Cross-correlation graph and power spectra of the patch recording (*black*) and the somatic fluorescence recording (*red*). **d** Confocal image of the recorded cell indicating fluorescence sampling locations (*red, pink, and green squares*)

522 patch electrode. (2) Fast imaging using a third dye showed
 523 that the peaks in calcium flux paralleled the oscillations in
 524 the electrical signal, although probably buffering of calcium
 525 by the dye reduced the frequency of the oscillations. (3) The
 526 mechanism behind both the imaged calcium oscillations and
 527 the parallel ramp-induced electrical oscillations was due to
 528 high threshold, voltage-dependent P/Q-type and N-type cal-
 529 cium channels. In this study, we found that Pf neurons
 530 produced measurable calcium transients in response to
 531 depolarizing current ramps even though all APs and synap-
 532 tic inputs were blocked. Beta/gamma oscillations present in
 533 the recorded electrical activity were also present in the
 534 fluorescent calcium activity signal, and these oscillations
 535 were evident in both the soma and proximal dendrites. This

is the first time that ramp-induced calcium oscillations have
 536 been described in the Pf using calcium-sensitive dyes. These
 537 oscillations have been reported previously in cortical, tha-
 538 lamic, hippocampal, and cerebellar cells. The advantage of
 539 visualizing these oscillations using dyes rather than only
 540 patch clamp recordings is that spatial differences can be
 541 detected, whereas patch clamp recordings only show aver-
 542 age oscillatory activity for the entire cell. These experiments
 543 used a variety of dyes in order to determine which work best
 544 for analyzing calcium oscillations. We focused on Fura, Bis
 545 Fura, and OGB1 because they presented the best results. We
 546 focused on using Fura and Bis Fura to provide the easiest
 547 and most accurate analysis of calcium concentrations due to
 548 their ratiometric properties. Both Fura and Bis Fura were
 549

Fig. 6 Oscillations measured simultaneously in a single dendrite. **a** Recording locations for each record in **(b)**. **b** Graded responses are shown in the calcium signal as it was measured simultaneously across 50 μM of proximal dendrite. Oscillations were evident along the dendrite with few gaps. **c** Graph showing the fluorescent trace area in relation to distance from the soma



550 used due to possibility that the higher affinity Fura would
 551 low-pass filter observed calcium dynamics. These dyes
 552 showed a moderate increase in calcium concentration in
 553 the dendrites with the peak of the calcium transient. OGB1

554 was used because it was best at visualizing the calcium
 555 oscillations with higher acquisition rates than those used
 556 for ratiometric analysis. This dye showed that, while indi-
 557 vidual oscillations could be visualized by the rapid imaging,

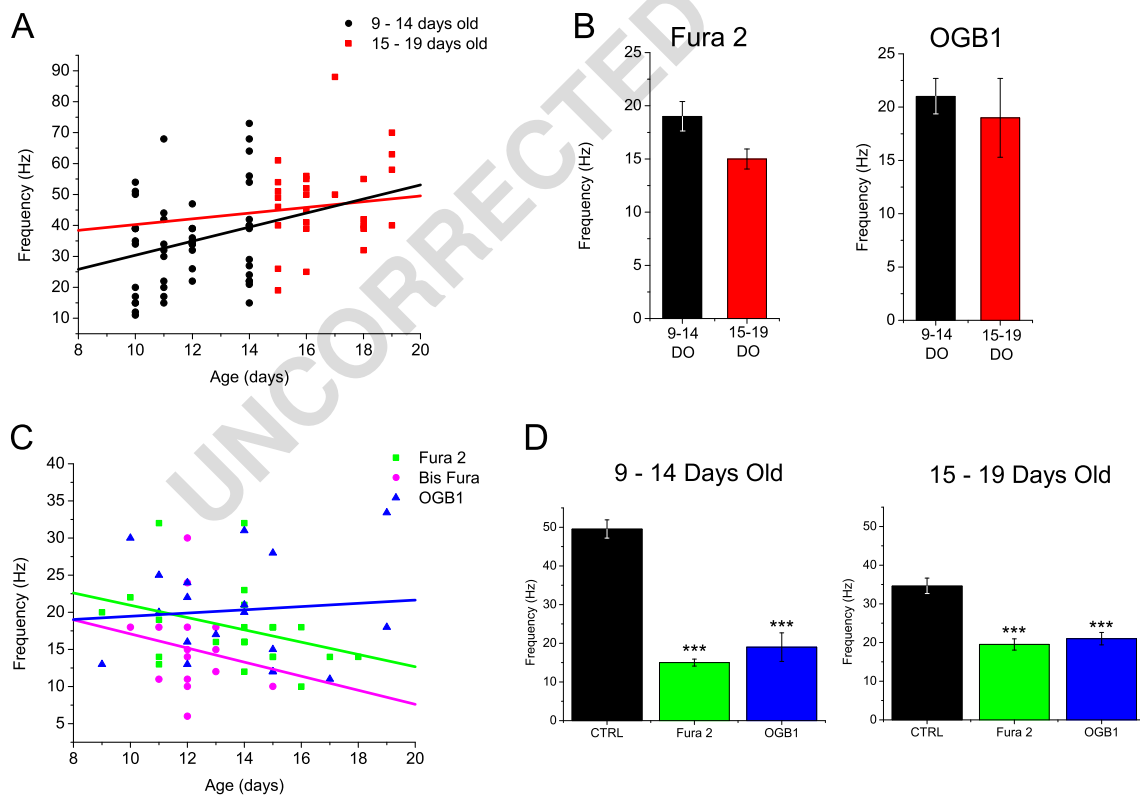


Fig. 7 Calcium dyes slowed the peak oscillation frequency in cells and confounded age-dependent frequency increases. **a** Scatter plot of the peak oscillation frequency of each control cell from 9–19 days old (DO). Cells were sub-divided into 9–14 DO (black) and 15–19 DO (red). Linear regression fits for each group (9–14 DO $R^2=0.24$; 15–19 DO $R^2=0.08$). **b** Bar graph showing average peak frequency for Fura 2 and OGB1 cells divided into 9–14 DO and 15–19 DO age groups (Fura 2 9–14 DO 19 ± 1.4 Hz; 15–19 DO 15 ± 0.94 Hz, $P > 0.05$; OGB1 9–14 DO 21 ± 1.7 Hz; 15–19 DO 19 ± 3.7 Hz, $P > 0.05$). Bis Fura was not

558 compared. **c** Scatter plot showing the peak oscillation frequency for
 559 each individual cell from 9–19 DO. Straight lines correspond to linear
 560 regression fits of each dye group (Fura 2 $R^2=-0.34$; Bis Fura $R^2=-0.2$;
 561 OGB1 $R^2=0.08$). **d** Bar graph comparing average peak frequency of
 562 Fura 2 and OGB1 dye groups to control cells of equivalent age. Both
 563 dye groups showed significantly lower frequencies regardless of age
 564 (CTRL 9–14 DO 34.6 ± 2.1 ; Fura 2 vs. CTRL, $P < 0.001$; OGB1 vs.
 565 CTRL, $P < 0.001$; CTRL 15–19 DO 49.5 ± 2.4 ; Fura 2 vs. CTRL,
 566 $P < 0.001$; OGB1 vs. CTRL, $P < 0.001$)

558 the frequency of the oscillations was reduced, perhaps due
559 to its $[Ca^{2+}]$ buffering capacity.

560 The mechanism behind the generation of these oscillations
561 has been shown to involve high-threshold voltage-
562 dependent P/Q- and N-type calcium channels [22, 23].
563 Herein we replicated our previous results using electrical
564 recordings, showed that oscillations present in calcium fluo-
565 rescence signals matched the oscillations in membrane po-
566 tential signals, and the use of AgA and CgTx allowed us to
567 eliminate both electrical oscillations and fluorescent calcium
568 transients in Pf neurons.

569 Our resting somatic calcium concentrations were similar
570 to resting concentrations reported in thalamic neurons [2, 4].
571 If we examine calcium concentrations in the dendrites, we
572 find slightly lower resting calcium concentrations, but still
573 within range in comparison to dendritic calcium concentra-
574 tions reported in hippocampal neurons and cortical neurons
575 (45–133 nM) [3, 11, 38]. In addition, intracellular dye
576 concentrations achieved in this study were capable of sig-
577 nificantly changing resting membrane potential, according
578 to their affinity to $[Ca^{2+}]$. These novel results suggest the
579 involvement of a Ca^{2+} -dependent potassium current in the
580 maintenance of resting membrane potential of Pf neurons.
581 Other work has shown that small-conductance type K^+
582 channels activate in conjunction with Ca^{2+} influx through
583 T-type calcium channels in thalamic reticular neurons [5].
584 This study did not control extraneous potassium currents
585 thus it is possible for uncontrolled calcium-mediated potas-
586 sium channel activation to alter the membrane potential,
587 which would explain the changes in resting membrane po-
588 tential levels described here. This may include other potas-
589 sium channels such as BK type potassium channels.

590 We show a moderate increase in calcium concentration in
591 the dendrites with the peak of the calcium transient. The
592 peak calcium concentration was lower than calcium concen-
593 trations seen in the dendrites of cortical neurons during
594 firing (383 nM) [3]. This was probably due to the lack of
595 firing in Pf neurons using synaptic blockers and TTX. More
596 specifically, we were recording oscillatory activity, thus the
597 calcium transients would be expected to be of lower ampli-
598 tude. It is possible that the depolarizing current ramps did
599 not elicit the maximum possible amplitude calcium tran-
600 sients. Also, caution must be used when interpreting abso-
601 lute calcium concentrations since the K_d value for each dye
602 can vary widely depending on intracellular conditions such
603 as temperature, ionic strength, and pH.

604 Early descriptions of the RAS suggested that it partici-
605 pates in “tonic” or continuous arousal [30]. Lesions of this
606 region eliminated tonic arousal [46], and it is possible that
607 PPN input to the Pf helps to maintain such activity. Using
608 OGB1, we were able to conduct high-speed calcium dye
609 recordings, showing calcium oscillations in Pf neurons. The
610 oscillations present in the somatic fluorescence records

611 closely matched the electrical patch clamp recordings,
612 which indicated a summation of calcium signals arriving
613 from the dendrites. The frequency and cross-correlation data
614 in turn support the contention that the oscillations seen in
615 the calcium signal were the same frequency as those ob-
616 served in the patch clamp record. Some time delays were
617 seen in the somatic fluorescence records, which may have
618 been due to the larger cytosolic volume of the soma and
619 kinetics of the dyes. We also observed calcium oscillations
620 in the proximal dendritic fluorescence recordings. Interest-
621 ingly, these oscillations may not exactly match oscillations
622 evident in the patch clamp recordings or the somatic fluo-
623 rescence recordings. Some oscillation peaks may be missing
624 or may be present in some dendrites, but not others. Also,
625 some peaks may exactly match the patch clamp recording
626 while others may be slightly out of phase. This may be
627 indicative of dendritic subdomains with some dendrites
628 having greater influence over the total calcium signal. Sep-
629 arate dendrites or regions within a single dendrite may
630 oscillate at slightly different phases, while all of the separate
631 oscillatory dendritic potentials are integrated in the record-
632 ing at the soma. We know that these oscillations are den-
633 dritic in origin due to the high depolarizing voltage, as
634 previously described [33]. While we were not able to visu-
635 alize distal dendrites and determine the precise origin of
636 each component of the full oscillatory signal, we can see
637 that different dendrites provide parts of the total signal and
638 that some dendrites may provide more than others.

639 Evoked calcium transients in Pf neurons showed a
640 distance-dependent incremental scaling with increments up
641 to 50 μ m. While the back propagation of calcium transients
642 decreased with distance from the soma, it is still possible
643 that large calcium accumulations may occur at distal sites.
644 This is similar to oscillations observed in “specific” TC
645 relay neurons. P/Q-type voltage-dependent calcium chan-
646 nels are found throughout the brain [16, 26]. More specifi-
647 cally these channels are found on the dendrites of the bushy
648 TC cells. The increase in calcium has been visualized in the
649 dendrites of these relay neurons using calcium imaging [33].
650 While we cannot determine the actual membrane potential
651 of the dendrites without actually clamping them (voltage
652 clamp of small dendrites leads to rapid dialysis of the
653 intracellular domain), the membrane potential is probably
654 lower than the ones seen at the somatic level during patch
655 recordings. This is due to total membrane capacitance be-
656 tween the electrode and the dendritic compartments. Unfortu-
657 nately, we were unable to visualize very distal compartments
658 using calcium dyes in Pf neurons due to their sparse, thin
659 dendrites. Very low dye concentrations in these distal dendrit-
660 ic compartments, coupled with the presence of few dendrites,
661 prevented us from obtaining recordings with adequate signal-
662 to-noise ratios. While we were unable to visualize the distal
663 compartments in Pf neurons, it may be possible to visualize

664 distal compartments in neurons with more compact morphol- 717
665 ogy such as PPN neurons. 718

666 Oscillations in the proximal dendrites appeared to be con- 719
667 tinuous across sequential sampling regions. We originally 720
668 expected to see localized regions of fluorescence with oscil- 721
669 lations, indicating specific regions of calcium channels. The 722
670 continuous presence of fluorescent oscillations suggests the 723
671 continuous presence of calcium channels across the proximal 724
672 dendrites. While this is possible, we must note that the intrin- 725
673 sic calcium buffering capabilities of calcium indicators can 726
674 accelerate the spatial spread of calcium signals. Typically, 727
675 calcium diffusion is spatially limited due to binding to large 728
676 endogenous calcium binding proteins. Conversely, calcium 729
677 buffers such as indicator dyes are relatively small, highly 730
678 mobile molecules that bypass calcium binding proteins and 731
679 allow unbinding at more distal locations [15]. Further exper- 732
680 iments will need to be conducted to analyze the spatial 733
681 distribution of voltage-dependent calcium channels 734
682 across dendritic sub-domains, possibly using higher mo- 735
683 lecular weight dextran-conjugated calcium indicators. 736
684 Bulk loading AM-ester versions of each dye may also 737
685 be a viable alternative for studying dendritic sub-domains 738
686 as well as providing better distal labeling with lower dye 739
687 concentrations. 740

688 The separate age groups of our control data showed that 741
689 oscillatory activity plateaued in the gamma band range in 742
690 older animals (15–19 days old), matching earlier studies [22, 743
691 23]. It should also be noted that this is the period when the 744
692 largest developmental decrease in REM sleep begins to level 745
693 off at the adult REM sleep levels [24]. Using the same com- 746
694 parison with the calcium dye groups, we did not see the same 747
695 developmental increase in frequency. The presence of the 748
696 calcium dye appeared to greatly vary the oscillation frequency 749
697 and thus confound efforts to study frequency-related results. 750
698 Our results show that the presence of calcium dyes decreased 751
699 the peak oscillation frequency in both young and old animals 752
700 in comparison to control data. This is probably due to the dye 753
701 acting as a calcium buffer as well as slowing calcium kinetics 754
702 [15, 38]. While the oscillation frequency may be slower, this, 755
703 however, does not prevent us from studying frequency data. 756
704 We should still be able observe relative changes in oscillation 757
705 frequency in response to drugs or other stimuli. Caution will 758
706 be necessary in interpreting any frequency data and much 759
707 larger experimental groups will be necessary to fully elucidate 760
708 questions regarding frequency effects. 761

709 Recently, new treatments for movement disorders such as 762
710 Parkinson's disease (PD) have centered on using deep brain 763
711 stimulation in the centromedian-parafascicular (CM/Pf) 764
712 complex of the thalamus [19]. Rodents possess mostly Pf 765
713 rather than the CM nucleus. While neurodegeneration of this 766
714 complex has been reported in PD patients [13], animal 767
715 models have shown extensive alterations in CM/Pf activity 768
716 [1, 9, 31, 32]. Moreover, strong antiparkinsonian benefits 769
770

717 have been obtained by applying high-frequency stimulation of 718
719 the Pf nucleus in rodents [19]. In this study, we showed that 720
721 calcium oscillations can be studied visually in the Pf nucleus 722
723 at the single cell level and confirmed that specific calcium 724
725 channels play a significant role in their generation. The im- 726
727 portance of this oscillatory activity may be considerable since 728
729 Pf neurons send widespread projections throughout the brain. 730
731 Thus, it is possible that novel pharmacological treatments can 732
733 be developed to target oscillatory output of the Pf nucleus for 734
735 treatment of certain movement disorders, rather than the use of 736
737 electrical stimulation of the CM/Pf complex. 738

739 The present findings present a viable methodology for 740
741 studying high-speed oscillations without the use of multi- 742
743 photon imaging systems. The advantage of using a wide 744
745 field-based imaging system is that we can simultaneously 746
747 record from many areas without having to account for 748
749 timing delays due to laser seek time. Wide field imaging is 749
750 particularly well suited for visualizing oscillations since all 751
752 imaging data must be acquired in a single run without 753
754 averaging (oscillations are almost never in phase from ramp 754
755 to ramp). Granted, wide field imaging has its limitations, in 755
756 particular, lower signal-to-noise ratio and potential signal 756
757 “bleed” from one area of interest to the next. Also, the 757
758 presence of high calcium dye concentrations modulates the 758
759 spatio-temporal characteristics limiting the variety of exper- 759
760 iments possible with this technique. This mainly means 760
761 careful analysis is necessary in interpreting results from 761
762 these experiments. Some of these problems can be resolved 762
763 with a multi-photon microscope, visualizing distal dendrites 763
764 in particular. Unfortunately, the cost and availability of 764
765 multi-photon microscopes are still limiting factors while 765
766 wide-field imaging systems have greater availability. We 766
767 used a combination of dyes in order to best elucidate the 767
768 various properties of subthreshold oscillations. While fewer 768
769 dyes may be used, we wanted to provide a broader basis for 769
770 researchers in the community to relate these techniques to 770
771 their experiments. We suggest that oscillatory activity gen- 771
772 erated in the Pf may help stabilize coherence related to 772
773 arousal and relay this activation to the cortex, thus providing 773
774 a stable activation state during waking. Much work is nec- 774
775 essary to support this speculation, but calcium imaging 775
776 techniques and localized calcium data such as those we 776
777 describe provide a useful stepping-stone in such investiga- 777
778 tions, especially since intracellular Ca^{2+} ions are known to 778
779 act as key second-messengers of intracellular pathways. 779
780

Acknowledgments The authors would like to thank Dr. Abdallah 762
763 Hayar for his assistance with calcium signal analysis. This work was 764
765 supported by USPHS award R01 NS020246, and by core facilities of the 765
766 Center for Translational Neuroscience supported by P20 GM104325 (to 766
767 EGR) and UL1 TR000039. In addition, Dr. Urbano was supported by 767
768 FONCyT, Agencia Nacional de Promoción Científica y Tecnológica 768
769 (<http://www.ifbyne.fcen.uba.ar/new/>): BID 1728 OC.AR. PICT 2008– 769
770 2019. None of the authors have a conflict of interest. 770

References

773 1. Aymerich MS, Barroso-Chinea P, Perez-Manso M, Munoz-Patino
774 AM, Moreno-Igoa M, Gonzalez-Hernandez T, Lanciego JL (2006)
775 Consequences of unilateral nigrostriatal denervation on the
776 thalamostriatal pathway in rats. *Eur J Neurosci* 23:2099–2108.
777 doi:10.1111/j.1460-9568.2006.04741.x

778 2. Budde T, Sieg F, Braunewell KH, Gundelfinger ED, Pape HC
779 (2000) Ca²⁺-induced Ca²⁺ release supports the relay mode of
780 activity in thalamocortical cells. *Neuron* 26:483–492

781 3. Cornelisse LN, van Elburg RA, Meredith RM, Yuste R,
782 Mansvelter HD (2007) High speed two-photon imaging of calci-
783 um dynamics in dendritic spines: consequences for spine calcium
784 kinetics and buffer capacity. *PLoS One* 2:e1073. doi:10.1371/
785 journal.pone.0001073

786 4. Coulon P, Herr D, Kanyshkova T, Meuth P, Budde T, Pape HC
787 (2009) Burst discharges in neurons of the thalamic reticular nuclei-
788 are shaped by calcium-induced calcium release. *Cell Calcium*
789 46:333–346. doi:10.1016/j.ceca.2009.09.005

790 5. Cueni L, Canepari M, Lujan R, Emmenegger Y, Watanabe M, Bond
791 CT, Franken P, Adelman JP, Luthi A (2008) T-type Ca²⁺ channels,
792 SK2 channels and SERCAs gate sleep-related oscillations in thalamic
793 dendrites. *Nat Neurosci* 11:683–692. doi:10.1038/nn.2124

794 6. Deschenes M, Bourassa J, Doan VD, Parent A (1996) A single-cell
795 study of the axonal projections arising from the posterior
796 intralaminar thalamic nuclei in the rat. *Eur J Neurosci* 8:329–343

797 7. Deschenes M, Bourassa J, Parent A (1996) Striatal and cortical
798 projections of single neurons from the central lateral thalamic
799 nucleus in the rat. *Neuroscience* 72:679–687

800 8. Eckhorn R, Bauer R, Jordan W, Brosch M, Kruse W, Munk M,
801 Reitboeck HJ (1988) Coherent oscillations: a mechanism of feature
802 linking in the visual cortex? Multiple electrode and correlation
803 analyses in the cat. *Biol Cybern* 60:121–130

804 9. Freyaldenhoven TE, Ali SF, Schmued LC (1997) Systemic admin-
805 istration of MPTP induces thalamic neuronal degeneration in mice.
806 *Brain Res* 759:9–17

807 10. Garcia-Rill E, Kezunovic N, Hyde J, Simon C, Beck P, Urbano FJ
808 (2013) Coherence and frequency in the reticular activating system
809 (RAS). *Sleep Med Rev*. In press. doi: 10.1016/j.smrv.2012.06.002

810 11. Goldberg JH, Tamas G, Aronov D, Yuste R (2003) Calcium
811 microdomains in aspiny dendrites. *Neuron* 40:807–821

812 12. Gray CM, Singer W (1989) Stimulus-specific neuronal oscillations
813 in orientation columns of cat visual cortex. *Proc Natl Acad Sci U S*
814 *A* 86:1698–1702

815 13. Henderson JM, Carpenter K, Cartwright H, Halliday GM (2000)
816 Loss of thalamic intralaminar nuclei in progressive supranuclear
817 palsy and Parkinson's disease: clinical and therapeutic implica-
818 tions. *Brain* 123(Pt 7):1410–1421

819 14. Herrero MT, Barcia C, Navarro JM (2002) Functional anatomy of
820 thalamus and basal ganglia. *Childs Nerv Syst* 18:386–404.
821 doi:10.1007/s00381-002-0604-1

822 15. Higley MJ, Sabatini BL (2012) Calcium signaling in dendritic
823 spines. *Cold Spring Harb Perspect Biol* 4:a005686. doi:10.1101/
824 cshperspect.a005686

825 16. Hillman D, Chen S, Aung TT, Cherksey B, Sugimori M, Llinas RR
826 (1991) Localization of P-type calcium channels in the central
827 nervous system. *Proc Natl Acad Sci U S A* 88:7076–7080

828 17. Iannuccielli E, Mompert F, Gellin J, Lahbib-Mansais Y, Yerle M,
829 Boudier T (2010) NEMO: a tool for analyzing gene and chromo-
830 some territory distributions from 3D-FISH experiments. *Bioinforma-*
831 *tics* 26:696–697. doi:10.1093/bioinformatics/btq013

832 18. Jeon D, Kim C, Yang YM, Rhim H, Yim E, Oh U, Shin HS (2007)
833 Impaired long-term memory and long-term potentiation in N-type
834 Ca²⁺ channel-deficient mice. *Genes Brain Behav* 6:375–388.
835 doi:10.1111/j.1601-183X.2006.00267.x

19. Jouve L, Salin P, Melon C, Kerkerian-Le Goff L (2010) Deep brain 836
stimulation of the center median-parafascicular complex of the 837
thalamus has efficient anti-parkinsonian action associated with 838
widespread cellular responses in the basal ganglia network in a 839
rat model of Parkinson's disease. *J Neurosci* 30:9919–9928. 840
doi:10.1523/JNEUROSCI.1404-10.2010 841

20. Jouvet-Mounier D, Astic L, Lacote D (1970) Ontogenesis of the 842Q4
states of sleep in rat, cat, and guinea pig during the first postnatal 843
month. *Dev Psychobiol* 2:216–239 844

21. Kao JP (1994) Practical aspects of measuring [Ca²⁺] with fluores- 845
cent indicators. *Methods Cell Biol* 40:155–181 846

22. Kezunovic N, Hyde J, Simon C, Urbano FJ, Williams DK, Garcia- 847
Rill E (2012) Gamma band activity in the developing 848
parafascicular nucleus. *J Neurophysiol* 107:772–784. 849
doi:10.1152/jn.00677.2011 850

23. Kezunovic N, Urbano FJ, Simon C, Hyde J, Smith K, Garcia-Rill 851
E (2011) Mechanism behind gamma band activity in the 852
pedunclopontine nucleus. *Eur J Neurosci* 34:404–415. 853
doi:10.1111/j.1460-9568.2011.07766.x 854

24. Llinas RR, Choi S, Urbano FJ, Shin HS (2007) Gamma-band 855
deficiency and abnormal thalamocortical activity in P/Q-type 856
channel mutant mice. *Proc Natl Acad Sci U S A* 104:17819– 857
1724. doi:10.1073/pnas.0707945104 858

24. Llinás RR, Grace AA, Yarom Y (1991) In vitro neurons in mam- 859Q5
malian cortical layer 4 exhibit intrinsic oscillatory activity in the 860
10- to 50-Hz frequency range. *Proc Natl Acad Sci U S A* 88:897– 861
901 862

25. Llinas RR, Steriade M (2006) Bursting of thalamic neurons and 863
states of vigilance. *J Neurophysiol* 95:3297–3308. doi:10.1152/ 864
jn.00166.2006 865

26. Luo M, Perkel DJ (1999) Long-range GABAergic projection in a 866
circuit essential for vocal learning. *J Comp Neurol* 403:68–84 867

27. Minamimoto T, Kimura M (2002) Participation of the thalamic 868Q6
CM-Pf complex in attentional orienting. *J Neurophysiol* 87:3090– 869
3101 870

28. Miura KRJ (2010) Bleach corrector. EMBL, Heidelberg 871

29. Moruzzi G, Magoun HW (1949) Brain stem reticular formation 872Q7
and activation of the EEG. *Electroencephalogr Clin Neurophysiol* 873
1:455–473 874

30. Orieux G, Francois C, Feger J, Yelnik J, Vila M, Ruberg M, Agid 875
Y, Hirsch EC (2000) Metabolic activity of excitatory parafascicular 876
and pedunclopontine inputs to the subthalamic nucleus in a rat 877
model of Parkinson's disease. *Neuroscience* 97:79–88 878

31. Parr-Brownlie LC, Poloskey SL, Bergstrom DA, Walters JR 879
(2009) Parafascicular thalamic nucleus activity in a rat model of 880
Parkinson's disease. *Exp Neurol* 217:269–281. doi:10.1016/ 881
j.expneurol.2009.02.010 882

32. Pedroarena C, Llinas R (1997) Dendritic calcium conductances 883
generate high-frequency oscillation in thalamocortical neurons. 884
Proc Natl Acad Sci U S A 94:724–728 885

33. Raeva SN (2006) The role of the parafascicular complex (CM-Pf) 886
of the human thalamus in the neuronal mechanisms of selective 887
attention. *Neurosci Behav Physiol* 36:287–295. doi:10.1007/ 888
s11055-006-0015-y 889

34. Rasband W (1997–2004) ImageJ National Institutes of Health, 890
Bethesda, Maryland, USA 891

35. Rhodes PA, Llinas R (2005) A model of thalamocortical relay 892Q8
cells. *J Physiol* 565:765–781. doi:10.1113/jphysiol.2004.070888 893

36. Sabatini BL, Oertner TG, Svoboda K (2002) The life cycle of 894
Ca(2+) ions in dendritic spines. *Neuron* 33:439–452 895

37. Segal M (1995) Imaging of calcium variations in living dendritic 896Q9
spines of cultured rat hippocampal neurons. *J Physiol* 486(Pt 897
2):283–295 898

~~38. Simon C, Kezunovic N, Williams DK, Urbano FJ, Garcia-Rill 899
E (2011) Cholinergic and glutamatergic agonists induce gam- 900
ma frequency activity in dorsal subcoeruleus nucleus neurons. 901~~

- 902 Am J Physiol Cell Physiol 301:C327–C335. doi:10.1152/
903 [ajpcell.00093.2011](https://doi.org/10.1152/ajpcell.00093.2011)
- Q10 904 39. Steriade M (1960) Unspecific systems of inhibition and facilitation of
905 potentials evoked by intermittent light. *J Neurophysiol* 23:602–617
- 906 40. Takahashi A, Camacho P, Lechleiter JD, Herman B (1999) Mea-
907 surement of intracellular calcium. *Physiol Rev* 79:1089–1125
- Q11 908 41. Thevenaz P, Ruttimann UE, Unser M (1998) A pyramid approach
909 to subpixel registration based on intensity. *IEEE Trans Image*
910 *Process* 7:27–41. doi:10.1109/83.650848
- 911 42. Uchitel OD, Protti DA, Sanchez V, Cherksey BD, Sugimori M,
912 Llinas R (1992) P-type voltage-dependent calcium channel medi-
913 ates presynaptic calcium influx and transmitter release in mamma-
914 lian synapses. *Proc Natl Acad Sci U S A* 89:3330–3333
- 928
43. Urbano FJ, Kezunovic N, Hyde J, Simon C, Beck P, Garcia-Rill E 915
(2012) Gamma band activity in the reticular activating system. 916
Front Neurol 3:6. doi:10.3389/fneur.2012.00006 917
44. Van der Werf YD, Witter MP, Groenewegen HJ (2002) The 918
intralaminar and midline nuclei of the thalamus. Anatomical and 919
functional evidence for participation in processes of arousal and 920
awareness. *Brain Res Brain Res Rev* 39:107–140 921
45. Watson RT, Heilman KM, Miller BD, King FA (1974) Neglect 922 Q12
after mesencephalic reticular formation lesions. *Neurology* 923
24:294–298 924
46. Ye M, Hayar A, Garcia-Rill E (2009) Cholinergic responses and 925
intrinsic membrane properties of developing thalamic parafascicular 926
neurons. *J Neurophysiol* 102:774–785. doi:10.1152/jn.91132.2008 927

UNCORRECTED PROOF

AUTHOR QUERIES

AUTHOR PLEASE ANSWER ALL QUERIES.

- Q1. Please check presentation of authors' affiliations if appropriate.
- Q2. Please check if section headings were assigned to appropriate levels.
- Q3. Please check figure captions if correctly presented.
- Q4. Ref. 20 was not cited anywhere in the text. Please provide a citation. Alternatively, delete the item from the list.
- Q5. Ref. 24 was not cited anywhere in the text. Please provide a citation. Alternatively, delete the item from the list.
- Q6. Ref. 27 was not cited anywhere in the text. Please provide a citation. Alternatively, delete the item from the list.
- Q7. Ref. 29 was not cited anywhere in the text. Please provide a citation. Alternatively, delete the item from the list.
- Q8. Ref. 35 was not cited anywhere in the text. Please provide a citation. Alternatively, delete the item from the list.
- Q9. Ref. 37 was not cited anywhere in the text. Please provide a citation. Alternatively, delete the item from the list.
- Q10. Ref. 39 was not cited anywhere in the text. Please provide a citation. Alternatively, delete the item from the list.
- Q11. Ref. 41 was not cited anywhere in the text. Please provide a citation. Alternatively, delete the item from the list.
- Q12. Ref. 45 was not cited anywhere in the text. Please provide a citation. Alternatively, delete the item from the list.